Ion-Sensitive Stainless Steel Vessel for All-Solid-State pH Sensing System Incorporating pH-Insensitive Diamond Solution Gate Field-Effect Transistors

Yu Hao Chang, Yutaro Iyama, Shuto Kawaguchi, Teruaki Takarada, Hirotaka Sato, Reona Nomoto, Kaito Tadenuma, Shaili Falina, Mohd Syamsul, Yukihiro Shintani, Junya Suehiro, and Hiroshi Kawarada, *Member, IEEE*

***Abstract*—An all-solid-state pH sensing system utilizing a stainless steel vessel (SUS304) and a pH-insensitive diamond solution-gate field-effect transistor (SGFET) is presented here to explain the interaction between stainless steel vessel and field-effect transistor (FET) pH sensors for the first time. A pH-sensitive ion-sensitive field-effect transistor (ISFET) was first used to show the change of the sensing behavior from 47.78 to −4.73 mV/pH when using an Ag/AgCl electrode and stainless steel vessel as the gate. This intriguing sensing behavior was investigated by developing large- and small-signal equivalent circuit models in a transistor circuit for both the Ag/AgCl and the stainless steel vessel gate. The result shows that the targeted ion change ΔQ_h corresponding to the pH sensitivity has been offset, which explains the phenomenon observed when using the pH-sensitive ISFET with the stainless steel vessel. We then hypothesize that combining a pH-insensitive device with the stainless steel vessel gate should show a pH sensitivity close to the Nernst response. To validate this, a pH-insensitive diamond SGFET was then fabricated and combined with the stainless steel vessel for pH measurements. The system demonstrates a high pH sensitivity at −54.18 mV/pH across a wide range of pH solutions (pH 2–12) and remains stable in elevated temperatures when measured with a potentiostat setup at 80 °C. The results also suggest that this all-solid-state sensing system has great potential to be used in the food and beverage industry where stainless steel is widely employed due to its excellent corrosion resistance, low cost, and high sensing capabilities.**

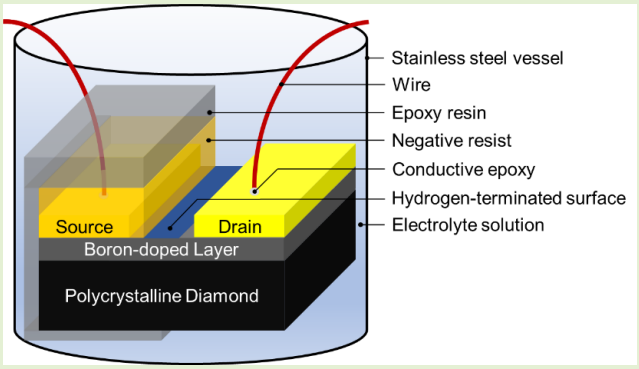

***Index Terms*— All-solid-state pH sensor, field-effect transistors (FETs), pH sensitivity, polycrystalline diamond, stainless steel.**

Manuscript received 3 February 2023; accepted 1 March 2023. Date of publication 20 March 2023; date of current version 1 May 2023. The associate editor coordinating the review of this article and approving it for publication was Dr. Chang-Soo Kim. *(Corresponding author: Yu Hao Chang.)*

Yu Hao Chang is with the Graduate School of Nanoscience and Nanoengineering, Waseda University, Tokyo 169-8555, Japan (e-mail: yu-hao.chang@ruri.waseda.jp).

Yutaro Iyama, Shuto Kawaguchi, Teruaki Takarada, Hirotaka Sato, Reona Nomoto, and Kaito Tadenuma are with the Graduate School of Fundamental Science and Engineering, Waseda University, Tokyo 169-8555, Japan.

Shaili Falina is with the Collaborative Microelectronic Design Excellence Centre, Universiti Sains Malaysia, Bayan Lepas, Penang 11900, Malaysia (e-mail: shailifalina@usm.my).

Mohd Syamsul is with the Institute of Nano Optoelectronics Research and Technology, Universiti Sains Malaysia, Bayan Lepas, Penang 11900, Malaysia (e-mail: nasyriq@usm.my).

Please see the Acknowledgment section of this article for the author affiliations.

Digital Object Identifier 10.1109/JSEN.2023.3257348

I. Introduction

STAINLESS steel has attracted much attention in the field of biosensing and food industry due to its fast response, low cost, and high sensing capabilities [1], [2], [3], [4], [5]. Several studies have reported the use of stainless steel (SUS304 and SUS316) for sensing applications and addressed some existing issues of glass sensors [6], [7], [8]. These glass sensors have been extensively used because of their stable and high sensing capability, high reliability, and intuitive operation. Nevertheless, these sensors are fragile and large in size and require constant recalibration due to contamination accumulation and liquid junction [9]. The stainless steel surface demonstrates close to ideal Nernstian pH sensitivity due to the films of mixed metal oxides on its surface. Upon further investigation, we found intriguing results when using the stainless steel as the gate in combination with either

diamond solution-gate field-effect transistors (SGFETs) with different surface functional groups or commercially available ion-sensitive field-effect transistors (ISFETs). While most reports focus on using a small piece of stainless steel for sensing or using the stainless steel as the backbone for other pH-sensitive coatings, we utilize a stainless steel vessel connected with the gate, thus the name stainless steel vessel gate, in this work. The advantages of this all-solid-state sensing system include a large surface sensing area, direct sensing on the stainless steel vessel surface, and excluding the use of any glass-related components (glass electrodes, glass beakers, and so on). This all-solid-state system also shows great potential to be used in the food and beverage industry where stainless steel vessels are widely used. In addition, the pH insensitivity of the diamond SGFET used is of great importance in this all-solid-state sensing system.

Diamond is suitable for biosensing and pH sensing applications due to its excellent properties including wide potential window, chemical inertness, and ease of surface modification. We have reported diamond SGFETs where the semiconductor surface was directly immersed in electrolyte solutions and the drain current was controlled by an electric double-layer capacitor at the diamond surface [10]. We have also reported diamond SGFETs utilizing various functional groups, including hydrogen, oxygen, nitrogen, and fluorine to achieve excellent pH sensing capabilities or complete pH insensitivity [11], [12], [13], [14], [15]. Like most ISFETs, a silver/silver chloride (Ag/AgCl) reference electrode has been commonly used as the gate electrode for diamond SGFETs. These glass electrodes have been widely used because of their lasting stability, fast response time, and a wide range of pH sensing capabilities. However, the risk of potassium chloride (KCl) internal solution leakage causing sample contamination, the problem concerning constant calibration required for maintaining the pH sensitivity, or breakage of the glass electrode have prevented it from being used in several industries [9]. One solution to this problem is to develop an all-solid-state pH sensing system, excluding the use of Ag/AgCl glass electrodes.

In the case of ISFETs, an all-solid-state pH sensing system consists of a pH-sensitive ISFET, a pH-insensitive reference FET (REFET), and a metal used for the quasi-reference electrode (QRE) [16], [17]. While various types of REFETs have been reported, achieving enough pH insensitivity for the all-solid-state pH sensing system to perform effectively while not sacrificing any pH sensing capability has been challenging. In the case of diamond SGFETs, hydrogen termination or fluorine termination incorporated diamond SGFETs have shown pH-insensitive results and are excellent potential candidates as REFETs for all-solid-state pH sensing systems. We have reported such a pH sensing system using a fluorine-terminated pH-insensitive diamond SGFET in combination with an oxygen-terminated diamond SGFET and platinum as the QRE [14]. The result shows moderate pH sensitivity and provides us insight on utilizing pH-insensitive diamond SGFETs as REFETs.

In this work, an all-solid-state pH sensing system is realized by utilizing pH-insensitive diamond SGFETs and a stainless steel vessel as the gate. We have reported a similar system utilizing pH-sensitive boron-doped diamond SGFETs with the stainless steel vessel [18]. However, much attention has been focused on the correlation between boron-doped diamond SGFETs and high temperatures. Here, large- and small-signal equivalent circuits are developed to explain the working mechanism of this all-solid-state pH sensing system. A potentiostat measurement is also conducted to observe the changes of the stainless steel vessel in elevated temperatures.

II. Material and Methods

Polycrystalline diamond substrates were used for fabricating the diamond SGFETs in this work, while the Si ISFETs were purchased from Winsense Company Ltd. [19], [20]. The diamond SGFET device design is similar to those reported in our previous reports and is shown in Fig. 1 [12], [15]. The polycrystalline diamond substrates were first cleaned in a mixture of nitric acid (HNO_3) and sulfuric acid (H_2SO_4) with a ratio of 1:3 at 200 °C for 30 min. The substrates were then cleaned for 10 min each in the order of deionized water, ethanol, acetone, ethanol, and deionized water in an ultrasonic washer to remove any organic residues. Hydrogen termination was conducted to the substrate surface under 600 °C in a hydrogen atmosphere at 20 torr for 30 min in a chemical vapor deposition (CVD) system. Contact lithography was used to form patterns on the substrate's surface. After depositing Au with an electron beam evaporator, source and drain electrodes were formed by lifting off the deposited pattern on the channel region. The Au electrodes were then encapsulated with negative resists (SU-8) except regions where wires were later attached to and bonded using conductive paste (Chemtronics). Finally, the entire device except the channel region was encapsulated using epoxy resin (Huntsman Advanced Materials) to prevent any leakage when measured in electrolyte solutions. The finalized hydrogen-terminated diamond SGFET device has a channel width $W = 5$ mm, channel length $L_g = 30$ μm, and $L_{gd} = L_{gs} = 10$ μm, where L_{gd} or L_{gs} refers to the distance between the end of a channel to the source or drain.

Carmody buffer solutions were prepared by mixing boric acid (BH_3O_3), citric acid monohydrate ($C_6H_8O_7$), and trisodium phosphate dodecahydrate ($Na_3PO_4{\cdot}H_2O$) solutions. The pH solutions from pH 2 to 12 were procured by measuring and calibrating the Carmody buffer solutions with a digital pH meter (Yokogawa Electric Corporation), which was carefully calibrated using a three-point calibration method using phthalate pH standard solutions. The pH sensitivity of the system was measured with a semiconductor device parameter analyzer (Keysight) with the LabVIEW program and was calculated based on the shift of V_{TH} for every pH solution. Two different gates were used: Ag/AgCl electrode and commercially available stainless steel vessel cup (SUS304). When using the Ag/AgCl electrode as the gate, the device and the electrode were both immersed in Pyrex beakers containing the corresponding pH solutions. In the case of using stainless steel vessel as the gate, the device was directly immersed in the stainless steel vessel containing the corresponding pH solutions, as shown in Fig. 2. A potentiostat measurement was used to observe the behavior of the stainless steel vessel in

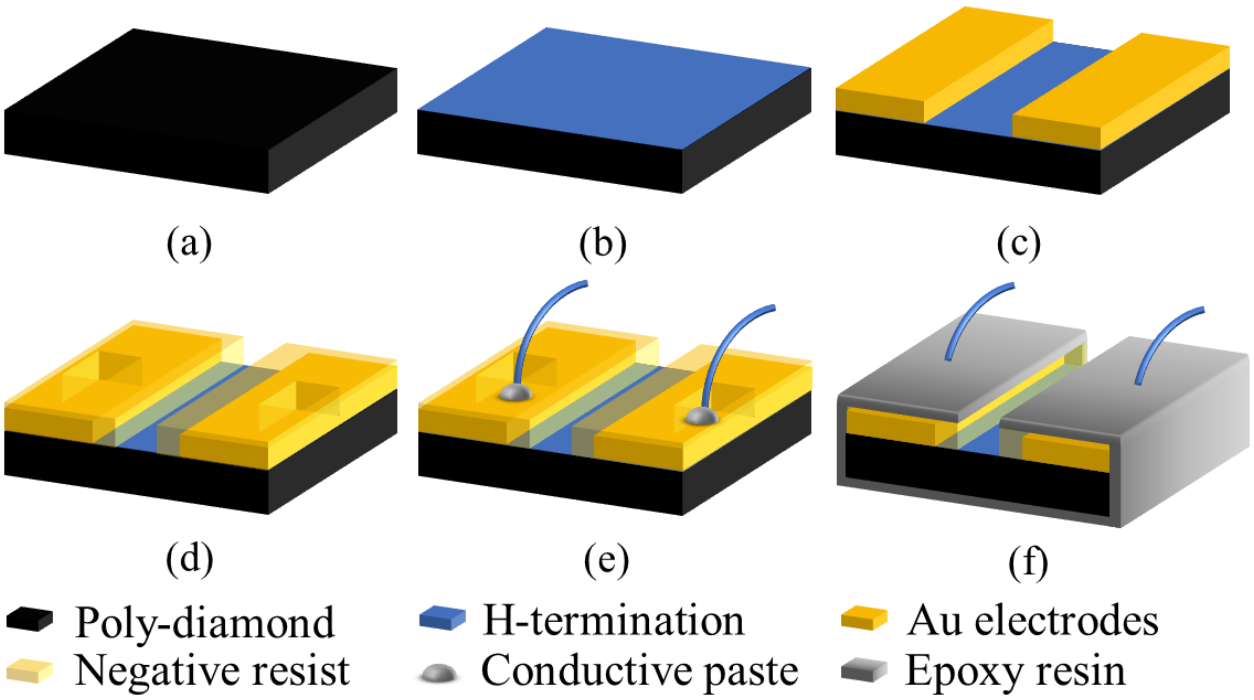

Fig. 1. Polycrystalline diamond SGFET device fabrication process. (a) Mixed acid cleaning using HNO_3 and H_2SO_4 at 200 °C for 30 min followed by organic cleaning in an ultrasonic washer. (b) Conducting hydrogen termination to the diamond surface in a hydrogen atmosphere at 20 torr for 30 min in a CVD system. (c) Forming the source and drain electrodes by depositing Au to the substrate's surface with an electron beam evaporator followed by lifting off the predeposited pattern on the channel region. (d) Encapsulating the source and drain region except areas reserved for wire connection. (e) Bond wires to the source and drain electrodes using conductive paste. (f) Encapsulate the entire device except the channel region to prevent leakage. The completed device has a channel width $W = 5$ mm, channel length $L_g = 30$ μm, and $L_{gd} = L_{gs} = 10$ μm, where L_{gd} or L_{gs} refers to the distance between the end of a channel to the source or drain.

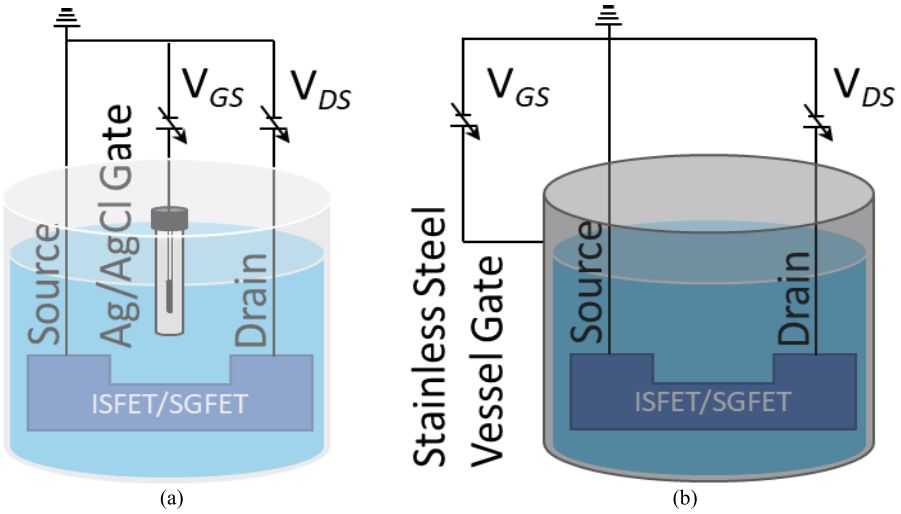

Fig. 2. pH measurement setup using an ISFET/SGFET with (a) Ag/AgCl electrode or (b) stainless steel vessel as the gate.

elevated temperatures. The Ag/AgCl glass electrode, Pt electrode, and stainless steel vessel were used as the reference electrode, counter electrode, and working electrode, respectively, while potentiostat measurements were taken from pH 2 to 12 at room temperature and 80 °C.

III. Results and Discussion

Fig. 3 shows the pH sensitivity of the ISFET when using two different gates. The ISFET shows a high pH sensitivity of −47.78 mV/pH when combined with the Ag/AgCl gate electrode. However, the pH sensitivity decreases to −4.73 mV/pH and shows no pH sensitivity when using the stainless steel vessel as the gate. The pH sensitivity difference between the two gates is around 53 mV/pH and is close to that of the Nernst response. The underlying mechanism of this sensing behavior can be explained using large- and small-signal equivalent circuit models in a transistor circuit [21]. The large-signal equivalent circuit is composed of a fixed term (dc) and a small-signal term (ac). Note that the ac term in this case is representative of the time-dependent part that is not

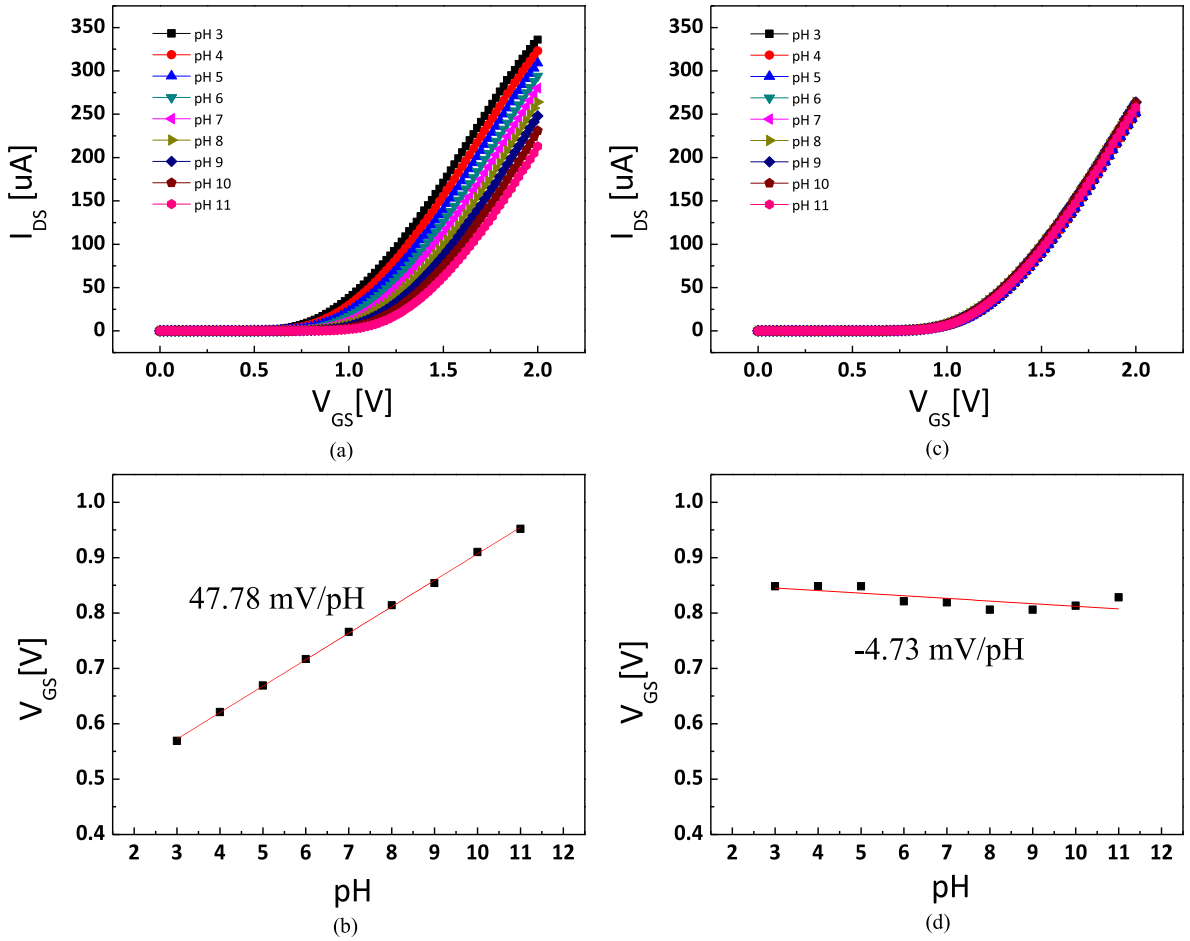

Fig. 3. pH measurement and pH sensitivity results of the ISFET at $V_{DS} = 1$ V when using (a) and (b) Ag/AgCl electrode or (c) and (d) stainless steel vessel as the gate. A high pH sensitivity of 47.78 mV/pH is obtained when using the Ag/AgCl electrode, but the pH sensitivity decreases drastically when using the stainless steel vessel as the gate.

necessary in the form of sinusoidal wave. Fig. 4 shows the large- and small-signal equivalent circuits of the Si ISFET or diamond SGFET system when using the Ag/AgCl electrode, where C_{EDL} is the electric double-layer capacity, C_i is the insulating film capacity in the Si ISFET or the inversion layer capacitance in the diamond SGFET, and ΔQ_h is the number of protons corresponding to the changes in pH solutions [10]. Since the ions in the pH solution are close to the surface of the insulating film, ΔQ_h is generated between C_{EDL} and C_i. Fig. 4(b) shows the large-signal equivalent circuit with a fixed voltage source V_{GS} (dc part) and a fluctuating small signal (ac part). When transforming the large-signal equivalent circuit to a small-signal equivalent circuit, voltage sources are shorted [Fig. 4(c)], and the two capacitors can be positioned in parallel. In the small-signal equivalent circuit, the electric charge ΔQ_h is divided between C_{EDL} and C_i in the form of parallel capacitance [Fig. 4(d)], and only ΔN accumulates charges in C_i. The equation for ΔN is shown as follows [22]:

$$\Delta N = -\frac{C_i \Delta Q_h}{C_{\mathrm{EDL}} + C_i} \tag{1}$$

where $\mathrm{C}_{\mathrm{EDL}}$ for Si ISFETs and diamond SGFETs is 5–10 μF/cm^2 and C_i in Si ISFETs and diamond SGFETs is approximately 0.1–0.5 μF/cm^2 with SiO_2 gate oxide ($\approx$10 nm in thickness) and 5 μF/cm^2, respectively [10]. Ci is considered to be constant since the carrier was enough at channel above V_T. In typical Si ISFETs, careful derivation of threshold voltage change is required as shown in the work by Xu et al. [23] due to having a gate insulator thicker than 10 nm and an additional passivation layer on top to prevent ion intrusion. For diamond SGFETs and very thin gate oxide ISFETs, however, the charge can be considered as a 2-D sheet on the channel since sensing happens directly on the channel surface. This allows the change in gate potential caused by changes in the pH solutions to simply be proportional to the number of carriers ($\Delta N \sim (\Delta Q_h)/(2)$) [10]. q$N$ (a large signal) is now the total charge of the FET channel and is composed of a first term (a fixed dc part at a certain V_{GS} point) where C_{EDL} and C_i are series capacitances in Fig. 4(b) and a second term (a small signal) with ΔN, and the equation can be expressed as follows [10]:

$$\begin{aligned} \mathrm{q}N &= -\frac{C_i C_{\mathrm{EDL}}}{C_{\mathrm{EDL}} + C_i}(V_{\mathrm{GS}} - V_T) + \Delta N \\ &= -\frac{C_i C_{\mathrm{EDL}}}{C_{\mathrm{EDL}} + C_i}(V_{\mathrm{GS}} - V_T) - \frac{C_i \Delta Q_h}{C_{\mathrm{EDL}} + C_i} \\ &= -\frac{C_i C_{\mathrm{EDL}}}{C_{\mathrm{EDL}} + C_i}\left\{V_{\mathrm{GS}} - \left(V_T - \frac{\Delta Q_h}{C_{\mathrm{EDL}}}\right)\right\}. \end{aligned} \tag{2}$$

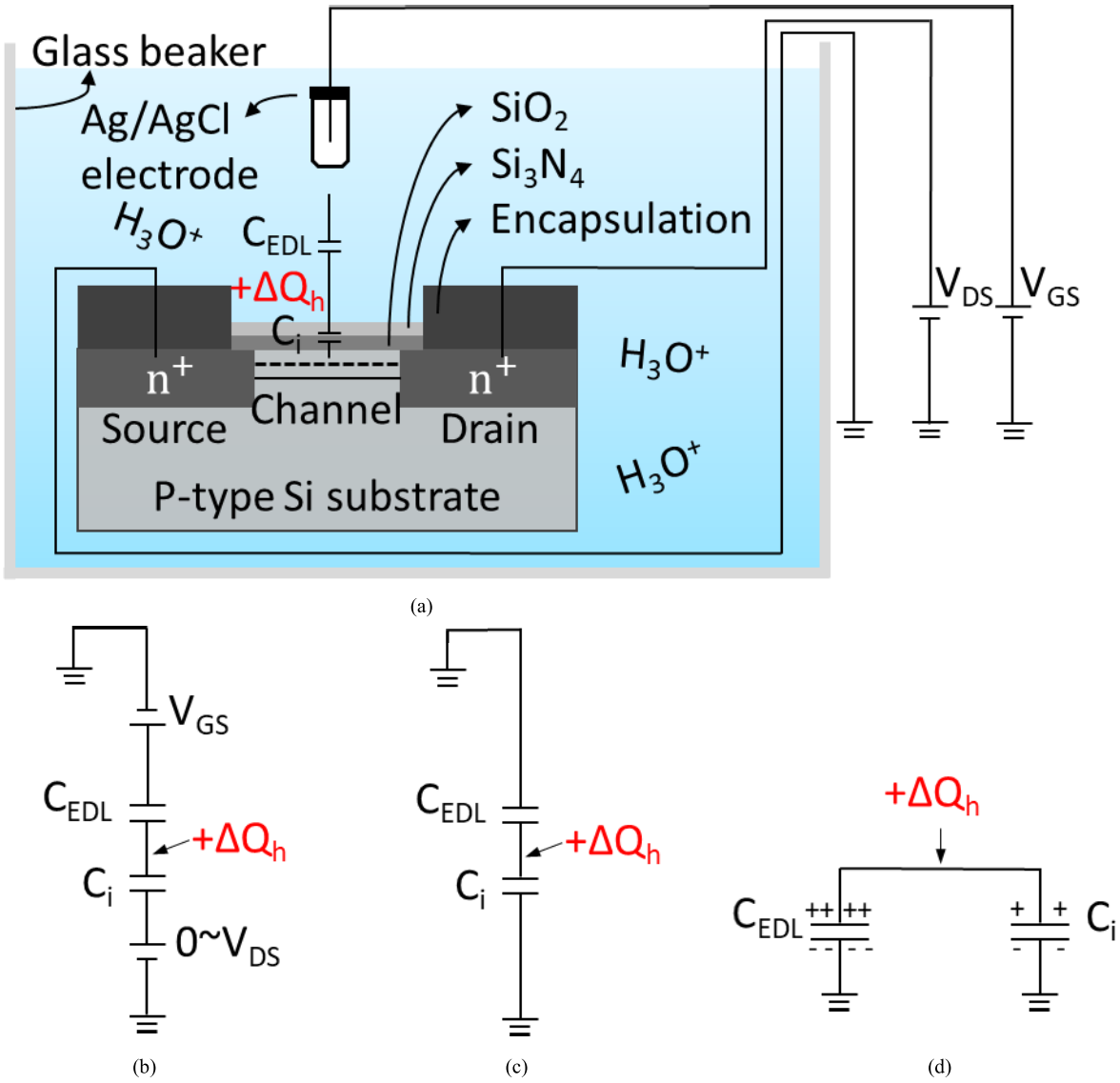

Fig. 4. Large- and small-signal equivalent circuits of the Si ISFET or diamond SGFET system when using the Ag/AgCl electrode [10]. (a) Illustration of the Si ISFET system when using the Ag/AgCl electrode as the gate. (b) Corresponding large equivalent circuit of (a). (c) Small-signal equivalent circuit when shorting the dc voltage sources. (d) Finalized small-signal equivalent circuits of the ISFET system showing ΔQ_h and electric charge distribution on the channel surface in the form of parallel capacitances between C_{EDL} and C_i.

When C_{EDL} is much greater than C_i, (2) can be approximated to the following:

$$\mathrm{q}N \approx -C_i \left\{ V_{\mathrm{GS}} - \left(V_T - \frac{\Delta Q_h}{C_{\mathrm{EDL}}} \right) \right\}. \tag{3}$$

Since ΔQ_h is inversely proportional to pH, meaning that the value of ΔQ_h is larger in low pH and smaller in high pH, the threshold voltage value increases and shifts to the positive side as pH increases. Fig. 5 shows the large- and small-signal equivalent circuits of the ISFET when using the stainless steel vessel. Since sensing happens directly on the surface of the stainless steel vessel in contact with the pH solutions, an electric double layer is considered for the vessel gate. The sensing area of the stainless steel vessel is attributed as k times larger than that of ISFET, and the capacity is expressed as $\mathrm{kC_{EDL}}$. The transformed small-signal equivalent circuit can be short-circuited of dc voltage sources because both sides of the circuit are grounded, and the potentials are the same. Since there are two signal sources, the analysis of V_T shift has been carried out by two superpositioned circuits with one signal source at each other, as shown in Fig. 6. The charges can be calculated by considering the independent two circuits separately when grounding either ΔQ_h or $\Delta k Q_h$. Fig. 6 shows the ΔQ_h grounded circuit where ΔN is expressed as follows [21]:

$$\Delta N = + \frac{C_i k \Delta Q_h}{k C_{\mathrm{EDL}} + C_i}. \tag{4}$$

The total charge can then be expressed as follows:

$$\begin{aligned} \mathrm{q}N &= -\frac{C_i k \mathrm{C_{EDL}}}{k \mathrm{C_{EDL}} + C_i} (V_{\mathrm{GS}} - V_T) + \Delta N \\ &= -\frac{C_i k \mathrm{C_{EDL}}}{k \mathrm{C_{EDL}} + C_i} (V_{GS} - V_T) + \frac{C_i k \Delta Q_h}{k \mathrm{C_{EDL}} + C_i} \\ &= -\frac{C_i k \mathrm{C_{EDL}}}{k \mathrm{C_{EDL}} + C_i} \left\{ V_{\mathrm{GS}} - \left(V_T + \frac{k \Delta Q_h}{k \mathrm{C_{EDL}}} \right) \right\}. \end{aligned} \tag{5}$$

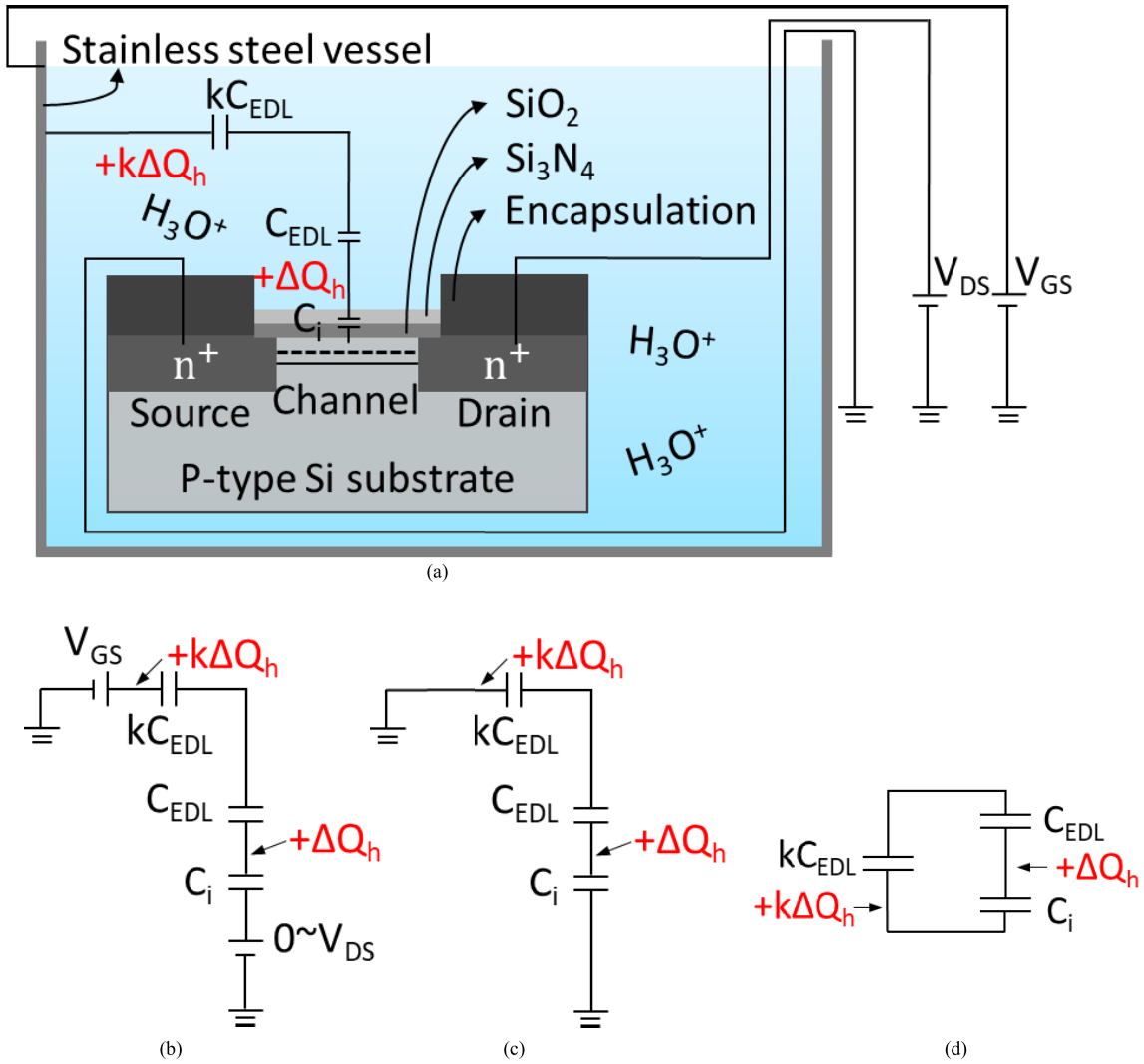

Fig. 5. Large- and small-signal equivalent circuits of the Si ISFET or diamond SGFET system when using stainless steel. (a) Illustration of the Si ISFET system when using the stainless steel vessel as the gate. (b) Corresponding large equivalent circuits of (a). (c) Small-signal equivalent circuit when shorting the dc voltage sources. (d) Finalized small-signal equivalent circuits of the Si ISFET system where $k\Delta Q_h$ is considered on the stainless steel vessel surface.

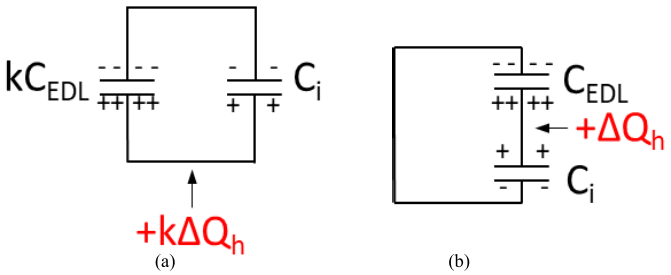

Fig. 6. Small-signal equivalent circuits of the ISFET vessel gate system shown in Fig. 5 when grounding either (a) ΔQ_h or (b) $k\Delta Q_h$. Fig. 5(d) can be obtained when superimposing these two small-signal equivalent circuits together.

When $\mathrm{kC_{EDL}}$ is much larger than C_i, (5) can be simplified and approximated to (6) as shown in the following:

$$\mathrm{q}N \approx -C_i \left\{ V_{\mathrm{GS}} - \left(V_T + \frac{\Delta Q_h}{C_{\mathrm{EDL}}} \right) \right\}. \tag{6}$$

In this case, the threshold voltage value decreases and shifts to the negative side as pH increases. When grounding $k\Delta Q_h$, since the sensitivity of the stainless steel vessel is not involved, the equation for this circuit is similar to (2) and (3) when using the Ag/AgCl electrode. By combining the approximated [(3) and (6)] calculated for the two grounded circuits, the ΔQ_h term corresponding to the pH sensitivity is canceled out as shown in the following equation:

$$\mathrm{q}N \approx -2C_i \left(V_{\mathrm{GS}} - V_T \right). \tag{7}$$

This explains why the combination of an ISFET and stainless steel vessel gate offsets the pH sensitivity. Therefore, we hypothesize that combining a pH-insensitive device with the stainless steel vessel gate should show a pH sensitivity close to the Nernst response. A hydrogen-terminated diamond SGFET was used as the pH-insensitive device with the stainless steel vessel gate to test this hypothesis, as shown in Fig. 7. Fig. 8 shows the pH sensing results of the hydrogen-terminated diamond SGFET when using different gates.

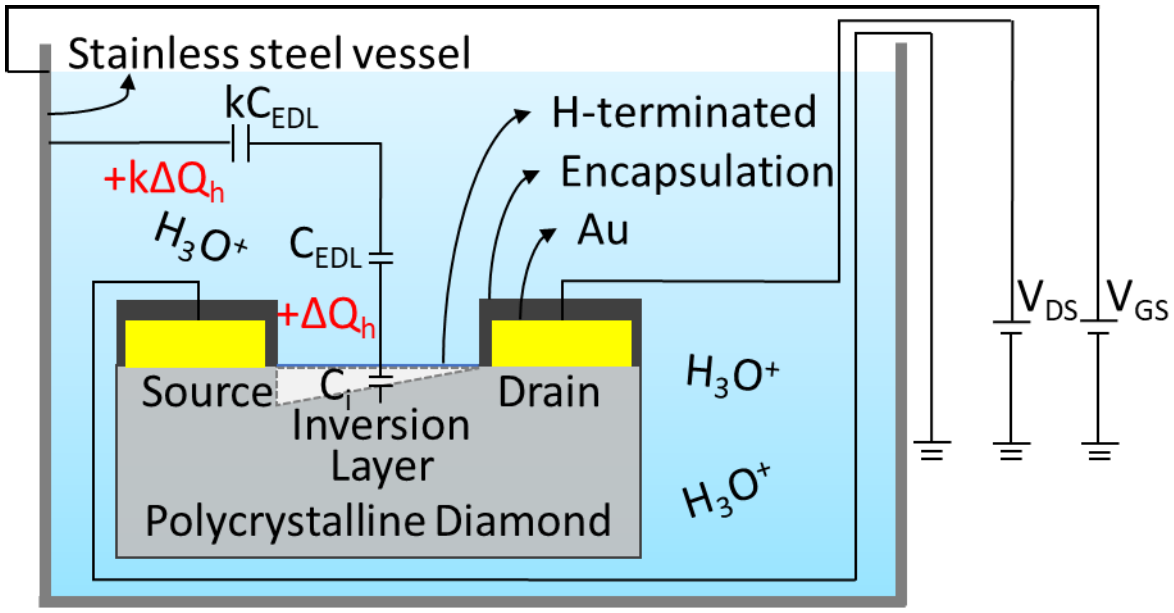

Fig. 7. Illustration of the fabricated hydrogen-terminated diamond SGFET device with stainless steel vessel as the gate.

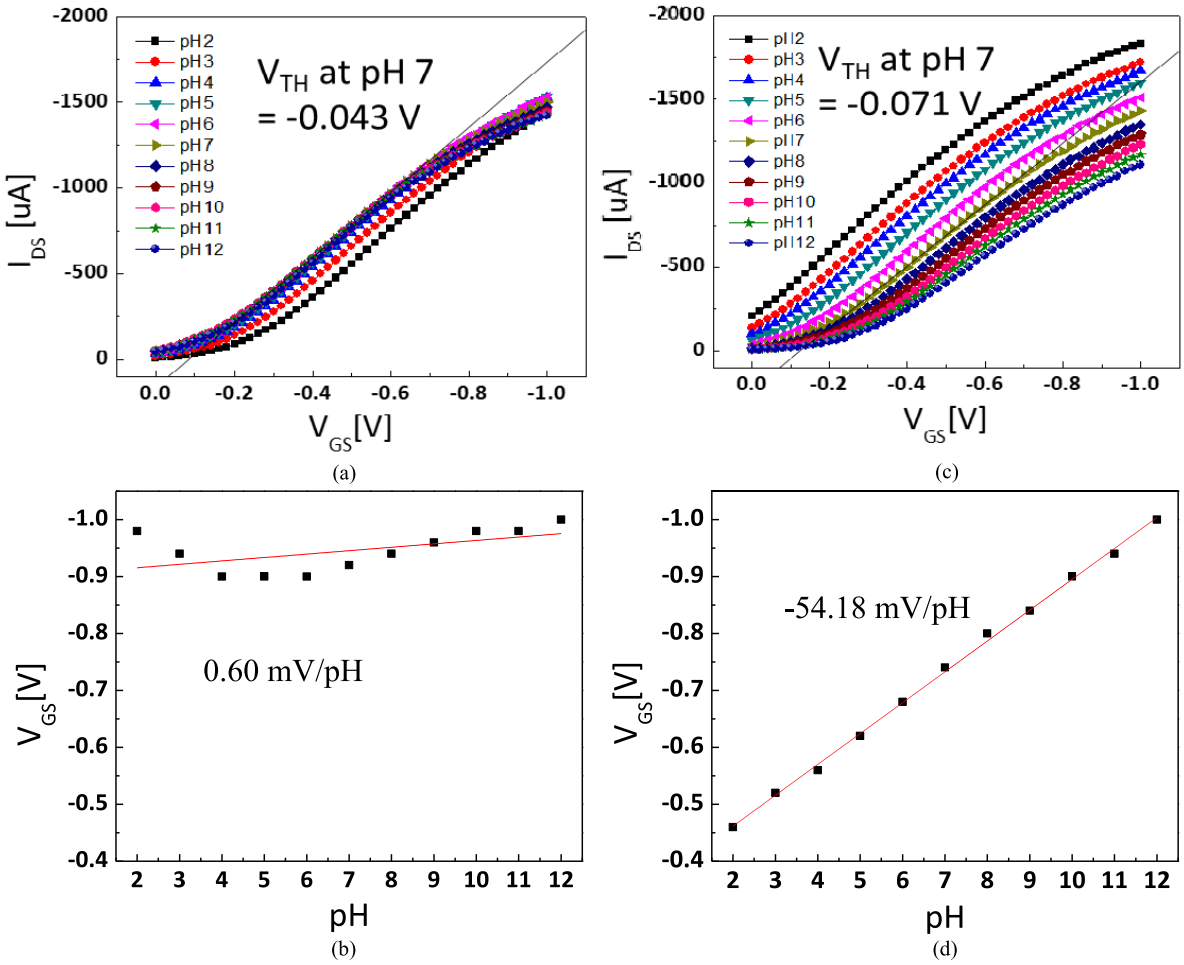

Fig. 8. pH measurement and pH sensitivity results of the H-terminated diamond SGFET versus (a) and (b) Ag/AgCl or (c) and (d) vessel gate. The sensitivity was investigated based on the shift of V_{TH} for every pH solution. The pH sensitivity can be approximated by first determining an I_{ds} value. V_{gs} of each pH at that I_{ds} is then calculated and plotted against pH. The pH sensitivity can then be calculated by finding the slope of the V_{gs} versus pH graph.

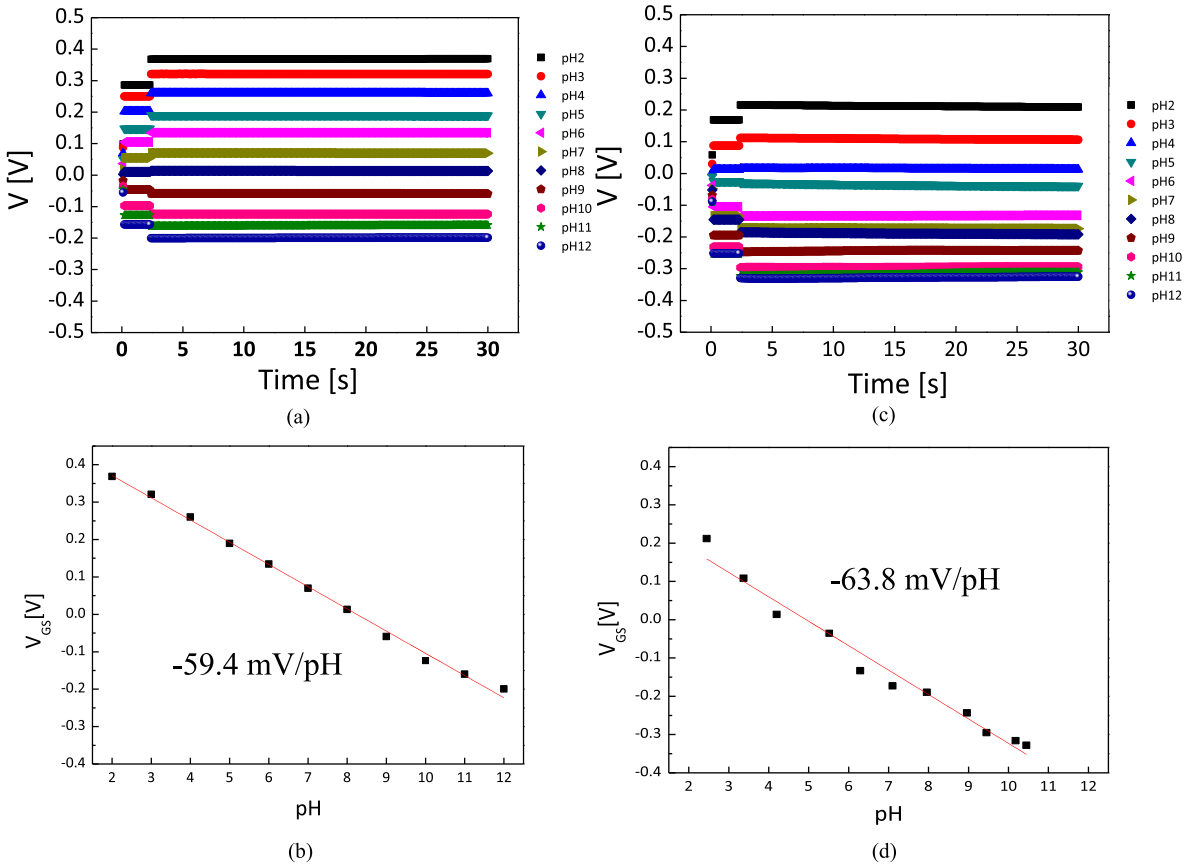

Fig. 9. Potentiostat measurement and pH measurement conducted to the stainless steel vessel (SUS304) at (a) and (b) room temperature and (c) and (d) 80 °C from pH 2 to 12.

The hydrogen-terminated device demonstrates close to zero pH sensitivity (0.60 mV/pH) when using Ag/AgCl as the gate. This pH-insensitive result is expected as explained in our previous report [8]. When using the stainless steel vessel as the gate, the system shows a high pH sensitivity at −54.18 mV/pH close to the Nernst response. The result confirms our hypothesis and shows excellent pH sensing capability. Clearly, a pH-insensitive SGFET, such as the hydrogen-terminated diamond SGFET used in this work, is preferred for obtaining a high pH sensitivity result when using the stainless steel vessel gate. While a detailed selectivity study on this all-solid-sensing system has yet to be conducted, a selectivity study on heat-treated stainless steel SUS304 and SUS316 as pH sensors has been reported by Nomura and Ujihira [1]. In their report, the heat treated stainless steel (SUS304) shows excellent hydrogen ion selectivity over a wide range of pH solutions (pH 1–13) coexisting with various alkali-metal ions including Li+, Na+, and K+. However, it shows an unstable pH response when immersed in 0.1- and 0.5-M NaCl solutions below pH 4. A similar selectivity study should be conducted in the future to understand the limitation of this all-solid-state sensing system with the untreated commercially available stainless steel SUS304. In addition, surface characterizations, including X-ray photoelectron spectroscopy (XPS), will help clarify whether there is any difference between the current commercially available stainless steel and others reported in the literature [1], [2]. Fig. 9 shows the potentiostat results and the pH sensitivity of the stainless steel vessel at room temperature and at 80 °C. The results suggest that the stainless steel vessel remains stable while demonstrating a high pH sensitivity at −59.4 and −63.8 mV/pH at room temperature and 80 °C, respectively. Due to partial channel oxidation of the hydrogen-terminated diamond SGFETs in elevated temperatures and limitations of the component used during our device fabrication, using the all-solid-state sensing system in higher temperatures has resulted in unstable measurements and inconsistent results. Alternative insensitive surface modifications, including fluorine termination that can withstand higher temperatures and heat-resistant wires, should be considered in future research.

IV. Conclusion

In summary, we have fabricated an all-solid-state pH sensing system using a hydrogen-terminated diamond SGFET and a stainless steel vessel as the gate. The results show a high pH sensitivity close to the Nernst response (−54.18 mV/pH). We have also shown pH sensing results of an ISFET connected to Ag/AgCl electrode or stainless steel vessel as the gate and explained the working mechanism of this system by using large- and small-signal equivalent circuits. The stainless steel vessel has shown excellent stability and pH sensitivity in both room temperature and 80 °C when measured in a potentiostat setup. Future research will focus on investigating the use of other pH-insensitive diamond SGFET such as the

fluorine-terminated diamond SGFETs with the stainless steel vessel gate, response time and the performance in elevated temperatures, and surface characterizations of the stainless steel vessel gate sensing system.

Acknowledgment

The authors thank the Research Organization for Nano & Life Innovation, the Materials Characterization Central Laboratory, and the Graduate Program for Power Energy Professionals (from MEXT WISE Program) at Waseda University for their support and encouragement.

Yukihiro Shintani is with the Department of Management Information Sciences, Chiba Institute of Technology, Narashino, Chiba 275-0016, Japan (e-mail: shintani@toki.waseda.jp).

Junya Suehiro is with the Department of Electrical Engineering, Faculty of Information Science and Electrical Engineering, Kyushu University, Nishi-ku, Fukuoka 819-0395, Japan (e-mail: suehiro@ees.kyushu-u.ac.jp).

Hiroshi Kawarada is with the Kagami Memorial Laboratory for Materials Science and Technology, Waseda University, Tokyo 169-0051, Japan (e-mail: kawarada@waseda.jp).

References

[1] K. Nomura and Y. Ujihira, "Response of oxide films on stainless steel as a pH sensor," *Anal. Chem.*, vol. 60, no. 23, pp. 2564–2567, Dec. 1988.

[2] T. Hashimoto, H. Kitabayashi, K. Ito, H. Nasu, A. Ishihara, and Y. Nishio, "Effect of heat-treatment on the pH sensitivity of stainless-steel electrodes as pH sensors," *Heliyon*, vol. 5, no. 3, Mar. 2019, Art. no. e01239.

[3] Z. B. Guzel-Seydim, A. K. Greene, and A. C. Seydim, "Use of ozone in the food industry," *LWT-Food Sci. Technol.*, vol. 37, no. 4, pp. 453–460, Jun. 2004.

[4] M. S. Jellesen, A. A. Rasmussen, and L. R. Hilbert, "A review of metal release in the food industry," *Mater. Corrosion*, vol. 57, no. 5, pp. 387–393, May 2006.

[5] Y. Wang et al., "Quantitative evaluation of susceptibility and shielding effects of nitinol, platinum, cobalt-alloy, and stainless steel stents," *Magn. Reson. Med.*, vol. 49, no. 5, pp. 972–976, May 2003.

[6] K. Nomura and Y. Ujihira, "Analysis of oxide layers on stainless steel (304, and 316) by conversion electron Mössbauer spectrometry," *J. Mater. Sci.*, vol. 25, no. 3, pp. 1745–1750, Mar. 1990.

[7] C. G. Zampronio, J. J. Rohwedder, and R. J. Poppi, "Development of a potentiometric flow cell with a stainless steel electrode for pH measurements. Determination of acid mixtures using flow injection analysis," *Talanta*, vol. 51, no. 6, pp. 1163–1169, 2000.

[8] T. Hashimoto, M. Miwa, H. Nasu, A. Ishihara, and Y. Nishio, "pH sensors using 3D-block metal oxide-coated stainless steel electrodes," *Electrochimica Acta*, vol. 220, pp. 699–704, Dec. 2016.

[9] W. Vonau and U. Guth, "pH monitoring: A review," *J. Solid State Electrochem.*, vol. 10, pp. 746–752, Sep. 2006.

[10] H. Kawarada and A. R. Ruslinda, "Diamond electrolyte solution gate FETs for DNA and protein sensors using DNA/RNA aptamers," *Phys. Status Solidi (A)*, vol. 208, no. 9, pp. 2005–2016, Sep. 2011.

[11] M. Tachiki et al., "Diamond nanofabrication and characterization for biosensing application," *Phys. Status Solidi (A)*, vol. 199, no. 1, pp. 39–43, Sep. 2003.

[12] S. Falina et al., "Role of carboxyl and amine termination on a boron-doped diamond solution gate field effect transistor (SGFET) for pH sensing," *Sensors*, vol. 18, no. 7, p. 2178, Jul. 2018.

[13] K.-S. Song, T. Hiraki, H. Umezawa, and H. Kawarada, "Miniaturized diamond field-effect transistors for application in biosensors in electrolyte solution," *Appl. Phys. Lett.*, vol. 90, no. 6, Feb. 2007, Art. no. 063901.

[14] Y. Shintani, M. Kobayashi, and H. Kawarada, "An all-solid-state pH sensor employing fluorine-terminated polycrystalline boron-doped diamond as a pH-insensitive solution-gate field-effect transistor," *Sensors*, vol. 17, no. 5, p. 1040, May 2017.

[15] Y. H. Chang et al., "Over 59 mV pH^{-1} sensitivity with fluorocarbon thin film via fluorine termination for pH sensing using boron-doped diamond solution-gate field-effect transistors," *Phys. Status Solidi (A)*, vol. 218, no. 5, Mar. 2021, Art. no. 2000278.

[16] P. Bergveld, "Development, operation, and application of the ion-sensitive field-effect transistor as a tool for electrophysiology," *IEEE Trans. Biomed. Eng.*, vol. BME-19, no. 5, pp. 342–351, Sep. 1972.

[17] K.-M. Chang, C.-T. Chang, K.-Y. Chao, and J.-L. Chen, "Development of FET-type reference electrodes for pH-ISFET applications," *J. Electrochem. Soc.*, vol. 157, no. 5, p. J143, 2010.

[18] S. Kawaguchi, R. Nomoto, H. Sato, T. Takarada, Y. H. Chang, and H. Kawarada, "pH measurement at elevated temperature with vessel gate and oxygen-terminated diamond solution gate field effect transistors," *Sensors*, vol. 22, no. 5, p. 1807, Feb. 2022.

[19] O. A. Williams, R. B. Jackman, C. Nebel, and J. S. Foord, "Black diamond: A new material for active electronic devices," *Diamond Rel. Mater.*, vol. 11, nos. 3–6, pp. 396–399, Mar. 2002.

[20] M. Syamsul, Y. Kitabayashi, D. Matsumura, T. Saito, Y. Shintani, and H. Kawarada, "High voltage breakdown (1.8 kV) of hydrogenated black diamond field effect transistor," *Appl. Phys. Lett.*, vol. 109, no. 20, Nov. 2016, Art. no. 203504.

[21] A. Sedra and K. Smith, *Microelectronic Circuits*, 6th ed. Oxford, U.K.: Oxford Univ. Press, 2009, pp. 400–401.

[22] A. Poghossian, A. Cherstvy, S. Ingebrandt, A. Offenhäusser, and M. J. Schöning, "Possibilities and limitations of label-free detection of DNA hybridization with field-effect-based devices," *Sens. Actuators B, Chem.*, vols. 111–112, pp. 470–480, Nov. 2005.

[23] G. Xu, J. Abbott, and D. Ham, "Optimization of CMOS-ISFET-based biomolecular sensing: Analysis and demonstration in DNA detection," *IEEE Trans. Electron Devices*, vol. 63, no. 8, pp. 3249–3256, Aug. 2016.

Yu Hao Chang received the B.A.Sc. degree in material science and engineering from the University of British Columbia (UBC), Vancouver, BC, Canada, in 2016, and the M.Eng. degree in nanoscience and nanoengineering from Waseda University, Tokyo, Japan, in 2019, where he is currently pursuing the Ph.D. degree in nanoscience and nanoengineering.

His research interests include diamonds, field-effect transistors, surface modifications, X-ray photoelectron spectroscopy (XPS), and sensors.

Mr. Chang received the Second Award for Best Student Speak in the 2018 Material Research Society Fall Meeting and Exhibit.

Yutaro Iyama received the B.Eng. and M.Eng. degrees in electronic and physical systems from Waseda University, Tokyo, Japan, in 2018 and 2020, respectively.

His research interests include diamonds, field-effect transistor sensors, surface modifications, seawater communications, and biosensing.

Shuto Kawaguchi received the B.Eng. and M.Eng. degrees in electronic and physical systems from Waseda University, Tokyo, Japan, in 2020 and 2022, respectively.

His research interests include diamonds, field-effect transistor sensors, boron doping, stainless steel, and biosensing in elevated temperatures.

Teruaki Takarada received the B.Eng. and M.Eng. degrees in electronic and physical systems from Waseda University, Tokyo, Japan, in 2020 and 2022, respectively.

His research interests include diamonds, field-effect transistors, and seawater wireless communications.

Mr. Takarada received the Best Poster Session Award at the 33rd Diamond Symposium in 2019 and the Nano Academy Award at the Nano Tech International Nanotechnology Exhibition and Conference in 2020.

Hirotaka Sato received the B.Eng. and M.Eng. degrees in electronic and physical systems from Waseda University, Tokyo, Japan, in 2021 and 2023, respectively.

He graduated as the top of his class in the School of Fundamental Science and Engineering at Waseda University. His research interests include diamonds, field-effect transistors, electrical circuits, and seawater wireless communications.

Mr. Sato was a recipient of the Nano Academy Award at the 2020 Nano Tech International Nanotechnology Exhibition and Conference and the Best Student Oral Presentation Award at the 2021 Materials Research Society Fall Meeting and Exhibit.

Reona Nomoto received the B.Eng. degree in electronic and physical systems from Waseda University, Tokyo, Japan, in 2022, where he is pursuing the M.Eng. degree in electronic and physical systems.

His research interests include diamonds, field-effect transistors, surface modifications, and biosensing.

Kaito Tadenuma received the B.Eng. and M.Eng. degrees in electronic and physical systems from Waseda University, Tokyo, Japan, in 2019 and 2021, respectively.

His research interests include diamonds, field-effect transistor sensors, boron doping, pH-insensitive surface modifications, biosensing, and seawater wireless communications.

Mr. Tadenuma received the Nano Academy Award at the 2020 Nano Tech International Nanotechnology Exhibition and Conference.

Shaili Falina received the bachelor's degree in electronic engineering from Universiti Malaysia Perlis (UniMAP), Arau, Malaysia, in 2009, and the Ph.D. degree in nanosciences and nanoengineering from Waseda University, Tokyo, Japan, in 2019, were focusing on diamond and graphene field-effect transistors for pH sensors.

Prior to her Ph.D., she was an RF Engineer at Motorola Solutions Penang, Penang, Malaysia, for five years working on radio transmitter section. Since 2020, she has been a Postdoctoral Fellow at Collaborative Microelectronic Design Excellence Center (CEDEC), Universiti Sains Malaysia (USM), Bayan Lepas, Malaysia, where she is appointed as a Lecturer. Her current research interests are printable and flexible electronics, electrochemical biosensors, and field-effect transistor biosensors.

Mohd Syamsul is a Researcher in the field of wide bandgap materials, specifically GaN, diamond, and carbon-related materials. He has made several contributions to the research of nanoelectronics, with a particular focus on developing diamond for biosensors and power devices. Previously, he worked as a Postdoctoral Researcher and a Doctoral Student at Waseda University, Tokyo, Japan, where he studied diamonds and their potential applications as power devices. Currently, he is a Senior Lecturer with the Institute of Nano Optoelectronics Research and Technology (INOR), Universiti Sains Malaysia (USM), George Town, Malaysia. He is also a Visiting Scientist at Waseda University, as well as a Research Fellow at the Institute of Nano Electronic Engineering (INEE), Universiti Malaysia Perlis (UniMAP), Arau, Malaysia. He is a certified Professional Technologist (Ts.), a certified Trainer, and a certified Lead Assessor ISO/IEC 17025:2017.

Yukihiro Shintani received the Ph.D. degree from Waseda University, Tokyo, Japan, in 2017, focusing on the development of all-solid-state ion sensors utilizing diamond field-effect transistors, and the M.B.A. degree from the University of Massachusetts, Lowell, MA, USA, in 2021.

He is a Professor with the Department of Social System Science, Chiba Institute of Technology, Narashino, Japan. His laboratory currently focuses on two research areas: social implementation of advanced technologies and technology management. In the advanced technology area, he mainly focuses on diamond semiconductors, the IoT, and robotic digital twins, while in the technology management area, he mainly focuses on innovation management and research and development organizational control. Prior to joining the university, he led research and development at several companies, including Yokogawa Electric Corporation, Tokyo, where he was responsible for the research and development of factory visualization technologies, and 3M, where he was responsible for the research and development of smart factories based on robotic digital twin technology.

Junya Suehiro received the B.Eng., M.Eng., and Ph.D. degrees in electrical engineering from Kyushu University, Fukuoka, Japan, in 1983, 1985, and 1991, respectively.

He was with Nippon Steel Company, Tokyo, Japan, from 1985 to 1988. Since April 1988, he has been with Kyushu University. He was a Visiting Professor at the University of Wales, Bangor, U.K., from 1997 to 1998. He is now a Professor and involved in research on bio and chemical sensors based on electrokinetics. He has authored or coauthored more than 200 articles, multiple conferences, and book chapters.

Dr. Suehiro is a member of the Institute of Electrical Engineers of Japan, the Institute of Electrostatics Japan, and the Japan Society of Applied Physics.

Hiroshi Kawarada (Member, IEEE) received the M.Eng. and Ph.D. degrees from the Graduate School of Science and Engineering, Waseda University, Tokyo, Japan, in 1978 and 1985, respectively.

From 1986 to 1990, he was an Assistant Professor at the Faculty of Engineering, Osaka University, Osaka, Japan, and an Associate Professor at the School of Science and Engineering, Waseda University, from 1990 to 1995. Since 1995, he has been a Professor at the School of Science and Engineering, Waseda University. He has authored or coauthored more than 300 articles, multiple conferences and review articles, and book chapters. His research interests include diamonds for power field-effect transistors and power inverters, superconductivity, seawater wireless communication, and biosensing.

Dr. Kawarada received the Commendation for Science and Technology Award from the Minster of Education, Culture, Sports, Science and Technology, Research Category, Japan.